THE EFFECT OF MOVING HEAT SOURCES UPON THE STRATIFICATION IN ROOMS VENTILATED BY DISPLACEMENT VENTILATION

Mats Sandberg, Magnus Mattsson
The National Swedish Institute for Building Research
Gävle, Sweden

SUMMARY

Moving heat sources, e.g. people, are present in rooms ventilated by displacement ventilation. The findings reported in this paper are from a basic study where the experiments were carried out in a physical model with water as fluid. Water was supplied at the bottom of the model along its whole width and was extracted at the top of the model. The plume flow was generated by a heat source that consisted of a rod heater. This heat source created a two layer stratification with lighter fluid floating above a heavier layer. A stratified system like this has a natural internal frequency and it is known that waves can exist at the interface between two layers of different densities.

The rod heater could be moved back and forth with a given stroke and frequency with the aid of a motor driven belt.

The following parameters were varied

- Length of the stroke of the moving heat source
- The frequency of the heat source oscillation
- Ventilation flow rate

The vertical temperature profile was recorded and the flow pattern was observed by adding fluorescent dye illuminated by a sheet of laser light.

The results show that the stratification may be affected in several ways by moving the heat source. Both lowering of the interface and standing waves occurred. It is therefore suggested to conduct systematic experiments in full scale of real rooms.

THE EFFECT OF MOVING HEAT SOURCES UPON THE STRATIFICATION IN ROOMS VENTILATED BY DISPLACEMENT VENTILATION

Mats Sandberg, Magnus Mattsson
The National Swedish Institute for Building Research
Gävle, Sweden

INTRODUCTION

The physical principles behind ventilation by displacement are based on the properties of stratified flow. Light-weight pollutants are prevented from being transported from the upper part of the room to the lower parts due to the density stratification caused by the vertical temperature profile in the room. The performance of this type of system is well documented in many research papers and case studies. However, in the majority of the papers the conditions were such that the heat source (people) were at rest.

The aim of this study is to systematically explore the influence of moving heat sources on the stratification. This is a basic study that will be followed by experiments conducted in full scale mock up of real rooms. This paper is a continuation of the previous studies carried out in the same model reported in [1] and [2] .

STATEMENT OF THE PROBLEM

Figure 1 shows a sketch of the experimental apparatus. In this paper we will consider the density stratification indicated as type a in Fig. 1. The space is filled with two layers of the same fluid but with different densities. A layer with lighter fluid is floating on a layer of heavier fluid. The layers are separated by an interface (internal boundary layer) and the heat source that creates the stratification is located below the interface.

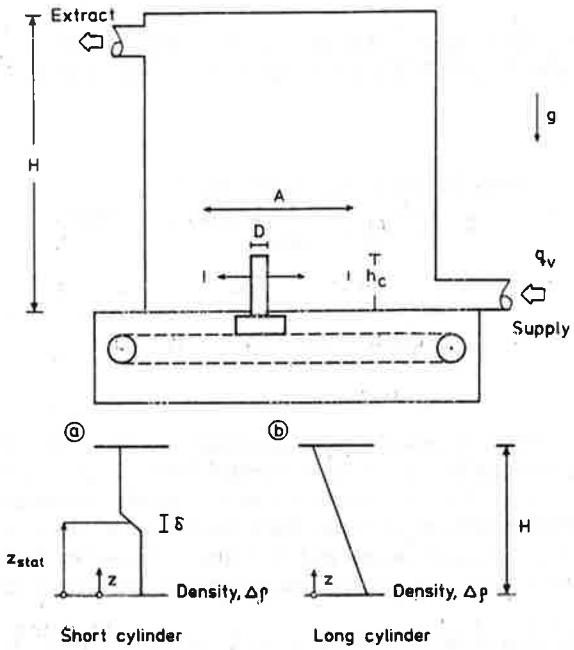

Fig. 1. Sketch of the model with a moving heat source

Location of the interface

The interface is the internal boundary layer at height z_{stat} that divides the space into two-zones. One lower zone with unidirectional flow directed upwards and an upper recirculation zone. Continuity dictates that the interface occurs at the height where the flow rate $q_p(z)$ in the flow generated by the heat source is equal to the supplied ventilation flow rate.

$$q_v = q_p(z_{stat}) \quad (1)$$

That is to say, at a given supply of ventilation air, the flow rate generated by the source governs the location of the interface. The above flow balance is based on continuity and must hold whether or not the heat source is moving. Therefore a change in height of the interface, when the heat source is moving, must be due to a change in flow rate in the plume flow from the heat source.

Thickness of the interface

The thickness, δ, is controlled by a balance between the thickening due to molecular diffusion and convective transport to the interface. The thickness is proportional to (κ is the molecular diffusivity)

$$\delta \sim (\kappa\tau)^{1/2} \quad (2)$$

where τ is the *finite* time scale over which the boundary layer develops.

Interfacial waves may be present and affect the thickness of the interface. The movement of the cylinder may change this time scale and thereby change the thickness.
The pertinent stability parameter for the interface is the Richardson number

$Ri = \frac{g\Delta\rho/\rho\delta}{U_c^2}$ based on the thickness of the interface or the Richardson number, Ri_0, based on the height (H - d) of the upper mixing zone (U_c is the velocity of source).

Internal frequency

Figure 2 shows a box filled with a fluid consisting of two layers with different densities. If the interface between the two layers is disturbed waves are produced.

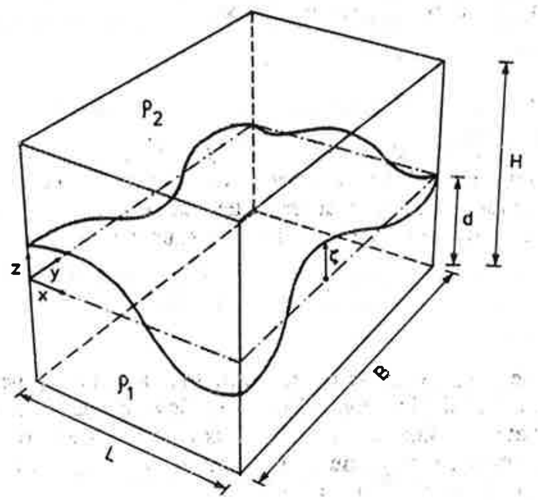

Fig. 2. A box filled with two layers of a fluid

After assuming irrotational motion in each layer, continuity of pressure across the interface and linearized boundary conditions applied at $z = 0$ instead of at $z = \zeta$, the *angular frequency* for the oscillation of the interface becomes

$$\omega_{m,n} = \left(\frac{g k_{m,n} (\rho_1 - \rho_2)}{\dfrac{\rho_1}{\tanh(k_{m,n} d)} + \dfrac{\rho_2}{\tanh(k_{m,n} (H-d))}} \right)^{1/2} \qquad [\frac{rad}{s}] \qquad (3)$$

where the *wavenumber* $k_{m,n}$ is

$$k_{m,n} = \left((\frac{n\pi}{L})^2 + (\frac{m\pi}{B})^2 \right)^{1/2} \qquad (4)$$

The possible wavelengths are

$$\lambda_{m,n} \equiv \frac{2\pi}{k_{m,n}} = \frac{2}{\sqrt{((\frac{n}{L})^2 + (\frac{m}{B})^2)}} \qquad (5)$$

The *period* τ of the wave is

$$\tau = \frac{2\pi}{\omega_{m,n}} \qquad (6)$$

The phase velocity $C \equiv \omega/k$ is a function of the wavenumber so the wave is dispersive because waves of different length propagate at different speeds. The group velocity $C_g \equiv \partial\omega/\partial k$ is equal to half the phase velocity.

When studying the effect of a moving heat source it is natural to at first consider the effect of the movement of a cold cylinder.

Cold cylinder

Oscillation of a body in form of a vertical circular cylinder with *diameter* D is characterised by its *stroke* A and *period of oscillation* T. The mean velocity of the cylinder is equal to $U_c = 2A/T$.

When the relative flow past a *cold* cylinder is undergoing harmonic oscillation the structure of the flow generated depends mainly on two parameters [3] :

- *Keugelan-Carpenter number* which is the ratio (A/D) between the stroke and the diameter of the cylinder
- *Stokes number*, $S = \frac{fD^2}{\nu}$, where $f = \frac{1}{T}$ is the frequency of the cylinder oscillation and ν is the kinematic viscosity of the fluid.

At small Keugelan-Carpenter number the flow generated is planar and symmetric whereas if the stroke is increased beyond a certain value flow separation occurs on the body surface and vortices are formed. Furthermore at small Keugelan-Carpenter number the flow induced is symmetrical and occurs in the direction of the body movement whereas at large Keugelan-Carpenter number the flow becomes non-symmetrical and three-dimensional.

Heated cylinder

We consider the heat source as a source of buoyancy with specific buoyancy flux B:

$$B = \frac{g\beta P}{\rho c_p} \qquad [\frac{m^4}{s^3}] \qquad (7)$$

where P is the total power output from the cylinder, β is coefficient of thermal expansion and c_p is the specific heat at constant pressure.

When the cylinder is at *rest* an axisymmetric plume is generated. The flow rate from an *axisymmetric* plume is

$$q_p = C(\alpha)B^{1/3}z^{5/3} \qquad (8)$$

where C is a constant dependent on the coefficient of entrainment, α.

Based on the specific buoyancy flux and the height h_c of the cylinder one can derive the following time scale.

$$\tau_c^B = (\frac{h_c^4}{B})^{1/3} \qquad (9)$$

This timescale is an estimate of the time it takes for a fluid particle to be transported from the base to the top of the cylinder. In relation to the period of oscillation,T, this timescale introduces two limits.

Fast oscillations $(T/\tau_c^B << 1)$

At fast oscillations the source is surrounded by fluid that previously has been heated by the source. One can therefore surmise the system to be equivalent to a heated solid bar with length A. Long strokes (A/D >> 1) may therefore give rise to a line source. The flow rate from a *line source* with length A and total specific buoyancy flux B is:

$$q_p = C'(\alpha)B^{1/3}A^{2/3}z \qquad (10)$$

For z < 10A the flow rate in an axisymmetric plume is less than the flow from a line source.

Slow oscillations ($T/\tau_c^B >> 1$)

At the combination of long strokes and slow oscillations there is an inflow towards the source of non-heated ambient fluid. It is natural to assume that induced flow rate, q_0, is proportional to the velocity of the source times the horizontally projected area.

$$q_0 = \gamma U_c h_c D \tag{11}$$

This amount of fluid is transported upwards along the cylinder and a plume flow is established at the top. The plume is bent (see Fig. 3) by the ambient velocity U_c. The plume trajectory is governed by the equation

$$\frac{dz}{dx} = \frac{W}{U_c} \tag{12}$$

After some distance the rising fluid loses its connection with the source which produced it and buoyant elements, *thermals* [4], are produced and a *bent over plume* is established. The characteristic length scale, Z_B, for a bent over plume is

$$Z_B = \frac{B}{U_c^3} \tag{13}$$

This is the *thermal rise*, i.e. the vertical distance the plume rises before it is affected by the ambient velocity.

The vertical velocity, W, in a two-dimensional thermal is proportional to $W \sim Z^{-1/2}$. Dimensional arguments give that the vertical flow rate becomes

$$q_p = C''q_0 \left(\frac{Z}{Z_B}\right)^{3/2} \qquad (Z > Z_B) \tag{14}$$

The effect of the curved trajectory has not been considered in the above formula.

EXPERIMENTAL RESULTS

The tests were carried out in a model built of plexiglas and with a side length equal to L = 0.5 m. Figure 1 shows a sketch of the model.

The supply temperature could be controlled very accurately by means of a microprocessor based PD controller. The buoyancy was generated by a heat source that consisted of a rod heater (Height = 96 mm, Diameter (D) = 20 mm). The experiments were carried out within the following parameter range (Re_D is the cylinder Reynolds number):

A/D = 0 - 19.9, Ri = 0.068 - 428, Ri_0 = 0.61 - 2010, Re_D = 240-610, S = 1.52 - 305

GENERAL INFLUENCE ON THE STRATIFICATION

Figure 3 shows a sequence of photos of a case where the stratification was affected by the movement of the source. At first equilibrium conditions are established with the source at rest. When the cylinder starts to move (A/D = 19.9) the density discontinuity begins to move downwards. As a result two fronts are developed. One front of warm (light) fluid moves downwards into colder (heavier) fluid. A second front is formed by the plume that now carries colder (heavier) fluid upwards and a front of cold fluid is formed on the top of the plume flow.

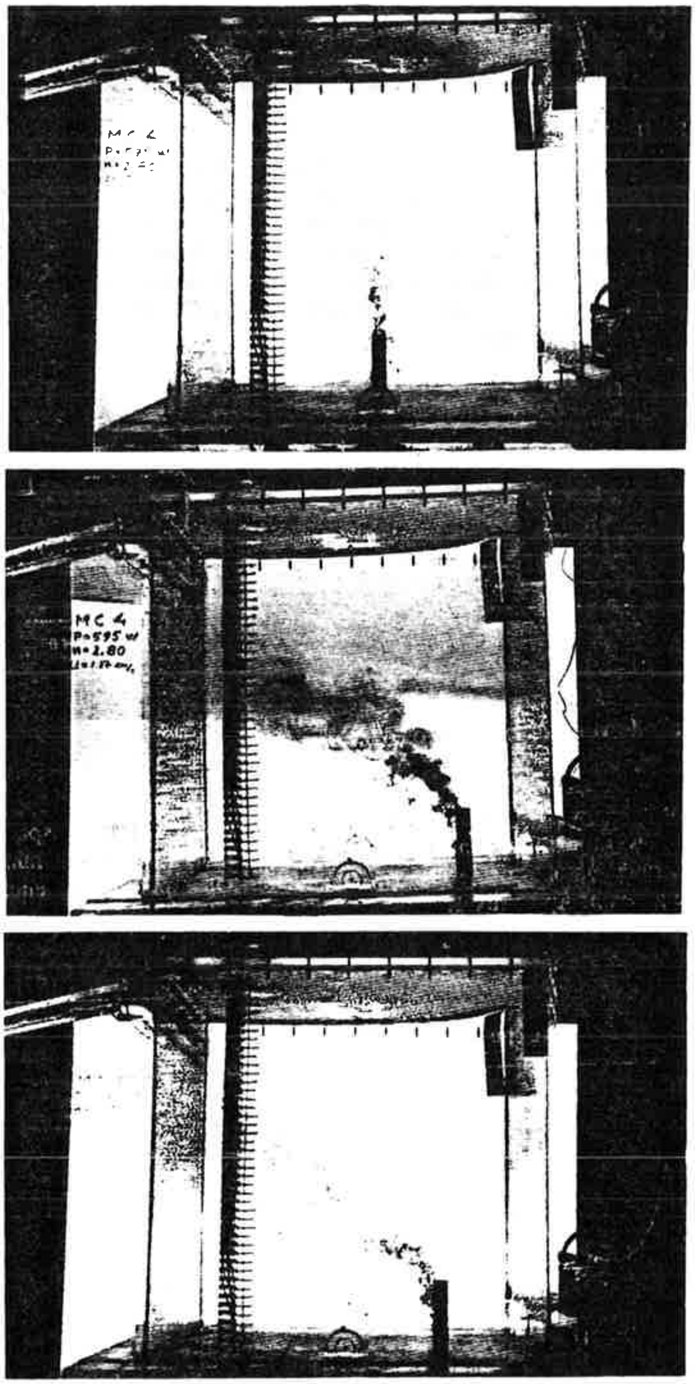

Fig. 3. Build up of upward moving front of heavier fluid (A/D = 19.9, T = 66 s, Z_B = 17 cm)
Top: Source at rest. Plume goes to the top of the enclosure
Centre: Source starts to move. Front is being formed
Bottom: Front has been established

Figure 4 shows a sketch of how the two fronts are developed.

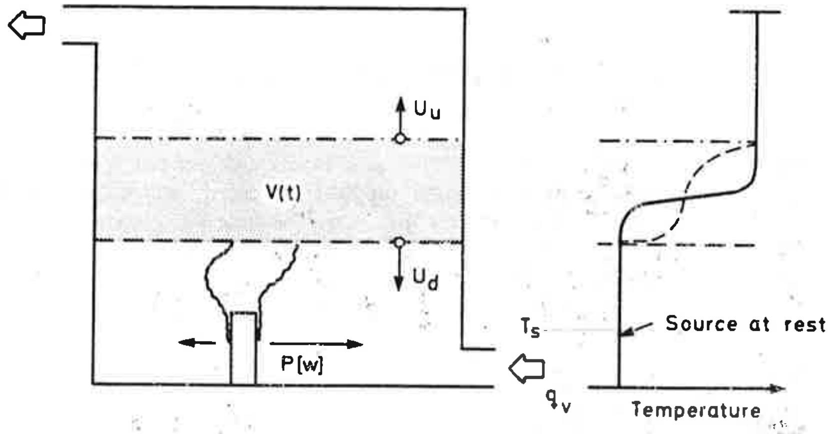

Fig. 4. Sketch of evolution of the two fronts

The speed, U_u, of the upward moving front is equal to the net vertical transport velocity (ventilation flow rate divided by the crossection). Figure 5 shows a numerical simulation of the time history of the temperature in the upper part of the enclosure. The equations are given in Appendix 1.

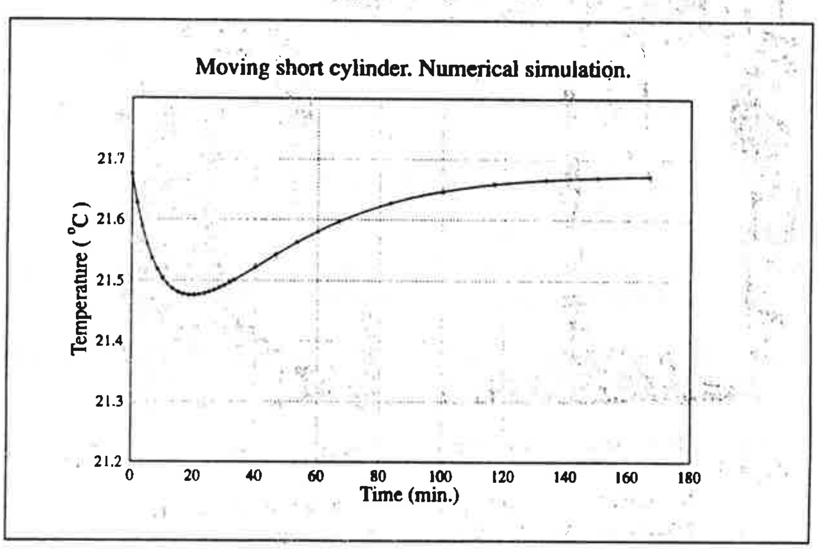

Fig. 5. Numerical simulation of the time history of temperature

When the source is stopped a reverse process is established. The density discontinuity moves upwards entraining lighter (warmer) fluid into the plume. Therefore the plume flow now penetrates the whole height and impinges upon the ceiling.

INFLUENCE ON THE PLUME FLOW

Figure 6 shows the recorded flow in the plume as a function of the height above the source. The data was obtained by varying the supply flow rate q_v and observing the height of the centre of density discontinuity (rel. (1)). The data are given in Appendix 2.

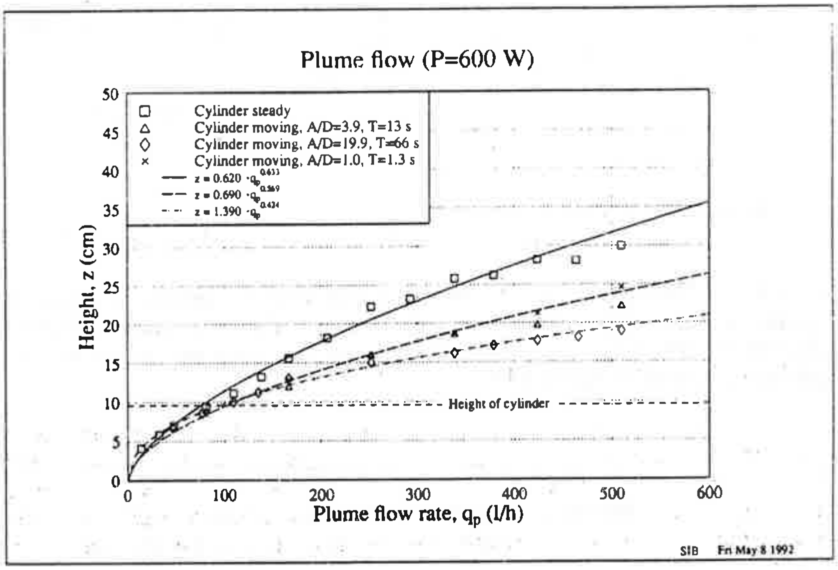

Fig. 6. Recorded plume flow versus height P = 600 W, $\tau_c^B = 6.5$ s

If one sets the induced flow rate as the flow rate at the top of the cylinder the measurements showed that at long strokes the factor γ in rel. (11) amounted to 1.14.

Figure 7 shows for long strokes (A/D = 19.9) the lowering of the interface as a function of the source oscillation frequency.

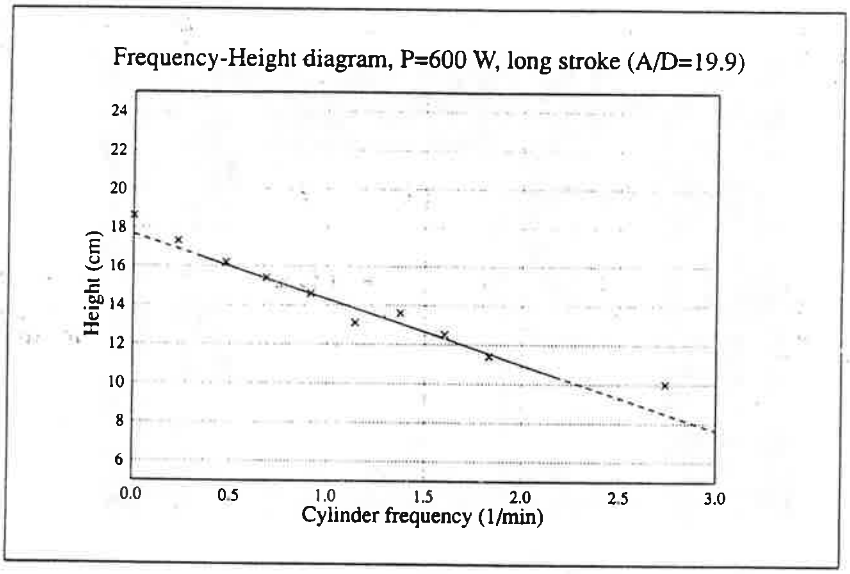

Fig. 7. **The height of the interface as a function the oscillation frequency of the source. Long strokes (A/D_c = 19.9). Constant heat supply (P = 600 W). q_v = 1 room-volume/h , τ_B^c = 6.5 s**

The relative change of height Δd/d was proportional to $Ri^{0.35}$.

The above results demonstrate that the lowering of the interface is dependent on the frequency of the oscillation. At long (A/D = 19.9) and medium strokes (A/D = 3.9) the lowering occurred at all frequencies. At short strokes (A/D = 1) the height of the interface was not influenced when the frequency of the oscillations were the same as previously. It order to obtain any effect it was necessary to increase the frequency of the oscillation.

INFLUENCE ON THE INTERFACE

Oscillation of the interface

Appendix 3 summarizes the result. The length of the stroke is measured to the centre of the heat source. The theoretical wave period is the period calculated from (7) for the values of m and n corresponding to the observed wave.

Although the moving source is located below the interface the plume flow introduces a coupling between the two layers. Hence oscillations are built up where the frequency of the source oscillation is close to the natural frequency of the system, see Fig. 8.

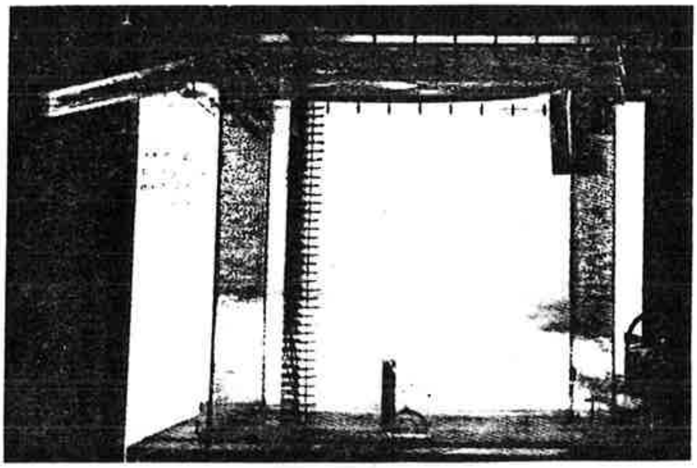

Fig. 8. Visualization of oscillating interface

The motion generated represents standing waves oscillating vertically between fixed nodes. Sloshing was generated in both directions and not only in the direction of the cylinder's movement. Figure 9 shows the type of standing waves that was observed when looking perpendicular to the direction of the cylinder's movement.

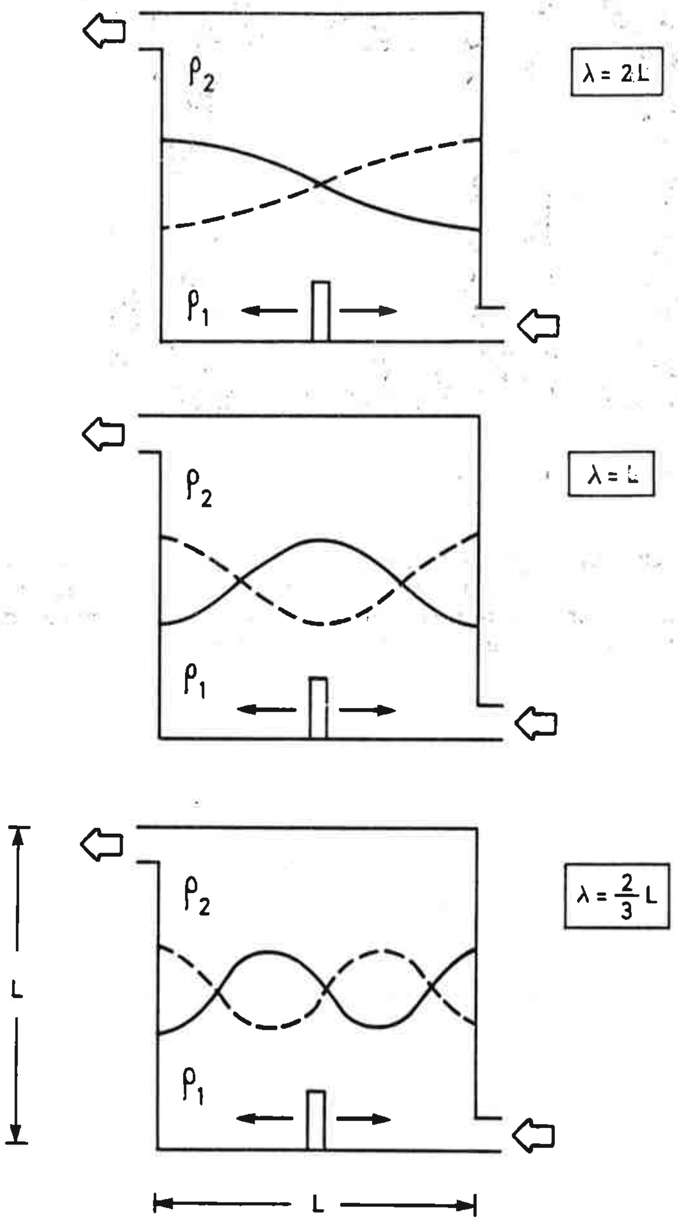

Fig. 9. Observed types of standing waves

CONCLUSIONS

Depending on the velocity of the heat (buoyancy) source a number of plume flow types are generated. At very low velocities axisymmetric plumes are generated, with increasing velocity the plume becomes bent-over and at high velocities the flow is entering the wake of the cylinder.

The movement of the source influenced the stratification in two ways.

- *Lowering the interface* between the lighter and heavier fluid. The lowering of the interface occurred in all cases with long strokes. This is caused by an increase of the flow rate in the plume. At a given cylinder stroke, a higher velocity (i.e. higher cylinder frequency) will lower the interface even more. The tests with very short cylinder strokes indicated that if the cylinder catches up with some previously heated fluid the interface will be less lowered.

- *Oscillation of the interface.* The oscillations occur despite the fact that the moving heat source is located below the interface. The motion generated represents standing wave oscillation between fixed nodes. Sloshing was generated in both directions and not only in the direction of the source movement. These oscillations occurred only for long stokes and when the frequency of the source was close to the system frequency introduced by the stratification. The mechanism that gives rise to the oscillations is probably the coupling between the two layers that the plume flow introduces.

ACKNOWLEDGEMENT

This work has been supported by a grant (No. 91-01826P) from NUTEK.

REFERENCES

[1] Sandberg, M., Lindström, S. "A model for ventilation by displacement". Proceedings Roomvent '87, Session 3, Stockholm 10-12 June 1987

[2] Sandberg, M., Lindström, S. "Stratified flow in ventilated rooms - a model study". Proceedings Roomvent'90, Paper 56, Norway, June 13-15, 1990

[3] Tatsuno, M., Bearman, P.W. "A visual study on the flow around oscillating circular cylinder at low Keugelan-Carpenter numbers and low Stokes number" J. Fluid Mech. 1990, Vol 211, pp 157-182

[4] Turner J.S. Buoyancy effects in fluids. Cambridge University Press 1973

APPENDIX 1

Conservation of heat within the volume, V(t), between the two fronts leads to a rate of mean temperature, T, change (Notation, see Fig. 4) within the volume:

$$\frac{d}{dt}(\rho C_p V T) = P + \rho C_p q_v T_s + \rho C_p A U_d T_s \qquad (1)$$

The rate of volume change is equal to

$$\frac{d}{dt}V = A(U_d + U_u) \qquad (2)$$

The downward moving front is caused by an increase of flowrate into the plume whereas the upwards moving front is governed by the net transport through the model

$$U_u = q_v/A \qquad (3)$$

Inserting (3) into (1) and (2) ($\Delta T = T - T_s$)

$$\frac{d}{dt}\Delta T = \frac{P}{\rho C_p V} - \frac{1}{V} q_v \Delta T - \frac{1}{V} A U_D \Delta T \qquad (4)$$

$$\frac{d}{dt}V = A U_D + q_v \qquad (5)$$

In order to be able to solve the equation the evolution of U_d must be known.

APPENDIX 2 Listing of experimental parameters in Fig. 6

$P = 600$ Watt, $\tau_c^B = 6.6$ s

ID	n	$\frac{A}{D}$	Ri	Ri_0	U_c	Cylinder period	S	Fundamental waveperiod m=1,n=0	$\frac{U_c}{C}$	Z_{stat}(=d)	δ	Z_B
	[rvol/h]	[1]	[1]	[1]	[cm/s]	[s]	[1]	[1]	[1]	[cm]	[cm]	[cm]
AQV510	4.07	-	-	-	-	-	-	85.3	-	30	4.88	-
AQV516	3.71	-	-	-	-	-	-	81.5	-	28.1	4.40	-
AQV511	3.37	-	-	-	-	-	-	72.7	-	28.2	4.80	-
AQV517	3.03	-	-	-	-	-	-	72.4	-	26.2	4.68	-
AQV512	2.70	-	-	-	-	-	-	69.3	-	25.8	4.76	-
AQV518	2.34	-	-	-	-	-	-	63.3	-	23.2	4.96	-
AQV513	2.02	-	-	-	-	-	-	58.4	-	22.2	5.08	-
AQV519	1.65	-	-	-	-	-	-	53.8	-	18.2	4.76	-
AQV514	1.33	-	-	-	-	-	-	46.2	-	15.2	5.04	-
AQV540	1.10	-	-	-	-	-	-	45.9	-	13.2	4.64	-
AQV515	0.873	-	-	-	-	-	-	39.9	-	11.1	3.65	-
AQV507	0.583	-	-	-	-	-	-	36.4	-	9.4	3.51	-
AQV508	0.258	-	-	-	-	-	-	29.7	-	5.8	5.72	-
AQV521	4.07	19.9	1.66	2.92	1.21	66	6.06	81.7	0.99	19.0	10.8	17
AQV529	3.71	19.9	1.74	3.11	1.21	66	6.06	77.8	0.94	18.2	10.2	17
AQV522	3.37	19.9	2.39	3.25	1.21	66	6.06	75.5	0.91	17.8	13.1	17
AQV530	3.03	19.9	1.69	3.51	1.21	66	6.06	71.6	0.87	17.2	8.29	17

APPENDIX 2 continuation

ID	n	A/D	Ri	Ri_0	U_c	Cylinder period	S	Fundamental waveperiod m=1,n=0	$\frac{U_c}{C}$	Z_{stat}(=d)	δ	Z_B
	[rvol/h]	[1]	[1]	[1]	[cm/s]	[s]	[1]	[1]	[1]	[cm]	[cm]	[cm]
AQV523	2.70	19.9	1.65	4.87	1.21	66	6.06	59.2	0.72	16.2	5.48	17
AQV524	2.02	19.9	2.25	4.62	1.21	66	6.06	59.5	0.72	15.0	7.30	17
AQV525	1.33	19.9	3.82	5.90	1.21	66	6.06	50.3	0.61	13.0	8.41	17
AQV531	1.10	19.9	3.99	6.34	1.21	66	6.06	46.5	0.56	11.2	7.06	17
AQV526	0.873	19.9	4.06	7.31	1.21	66	6.06	42.1	0.51	10.0	5.56	17
AQV527	0.583	19.9	6.24	8.67	1.21	66	6.06	37.3	0.45	8.6	6.19	17
AQV528	0.46	19.9	10.0	12.3	1.21	66	6.06	29.9	0.36	6.8	5.52	17
AQV603	4.07	1.0	0.068	0.61	3.05	1.31	305	79.7	2.43	24.6	2.78	1.1
AQV601	3.37	1.0	0.115	0.61	3.05	1.31	305	73.9	2.26	21.2	3.97	1.1
AQV109	2.70	1.0	0.136	0.58	3.05	1.31	305	72.0	2.20	18.7	4.37	1.1
AQV602	2.02	1.0	0.173	0.76	3.05	1.31	305	59.6	1.82	16.0	3.65	1.1
AQV604	1.33	1.0	0.219	0.91	3.05	1.31	305	50.4	1.54	12.8	3.06	1.1
AQV605	0.583	1.0	0.84	1.26	3.05	1.31	305	38.6	1.18	8.4	5.56	1.1

APPENDIX 3 Oscillation of interface. Listing of experimental parameters

P = 600 Watt, $\tau_c^B = 6.5$ s, n = 2.02 room-volumes/h (Except AQV107)

ID	$\frac{A}{D}$ [1]	Ri [1]	Ri_0 [1]	U_c [cm/s]	Cylinder period [s]	S [1]	Measured waveperiod (L=0.5 m)	Measured amplitude [cm]	Fundamental waveperiod [s] m=1, n=0	Measured waveperiod [s]	Theoretical waveperiod [s]	$\frac{U_c}{C}$ [1]	Z_{stat}(=d) [cm]	δ [cm]	Z_B [cm]
AQV579	19.9	13.9	80.3	0.30	263.0	1.52	-	-	60.5	-	-	0.182	17.3	2.98	1140
AQV571	19.9	5.32	18.8	0.60	131.5	3.64	-	-	61.1	-	-	0.366	16.7	4.56	143
AQV572	19.9	3.66	7.77	0.91	87.7	4.6	L	4	61.4	43.8	40.1	0.56	15.4	7.22	41
AQV573	19.9	2.54	4.17	1.21	65.8	6.1	2 · L	5.5	61.9	65.8	61.9	0.751	14.6	8.85	17
AQV574	19.9	1.65	2.41	1.51	52.6	7.6	2 · L	2	62.2	52.6	62.2	0.956	13.1	8.97	9.0
AQV575	19.9	1.08	1.74	1.81	43.8	9.1	2/3 · L	6.5	62.7	43.8	40.4	1.14	13.6	8.45	5.2
AQV576	19.9	0.78	1.17	2.11	37.6	10.6	-	-	63.9	-	-	1.35	12.5	8.25	3.3
AQV577	19.9	0.51	0.820	2.41	32.9	12.2	-	-	65.2	-	-	1.57	11.4	7.06	2.2
AQV578	19.9	0.23	0.317	3.63	21.9	18.2	-	-	67.3	-	-	2.44	10.0	7.22	0.64
AQV587	1	.428	2010	0.061	66.0	6.1	-	-	60.3	-	-	0.037	17.9	3.81	-
AQV107 (n = 2.70)	1	1.30	6.71	1.03	3.9	103	-	-	68.5	-	-	0.705	22.9	4.44	-
AQV602	1	0.164	0.719	3.05	1.31	305	-	-	61.2	-	-	1.87	18.0	3.65	-